Eur. Phys. J. Appl. Phys. (2013) 64: 10405
DOI: 10.1051/epjap/2013130012

THE EUROPEAN PHYSICAL JOURNAL APPLIED PHYSICS

Regular Article

Preparation of mesoporous MgO: phenomena occurred during the calcination*

Pham Thanh Huyen[1], Emanuela Callone[2], Renzo Campostrini[2], Giovanni Carturan[2], Tran Thi Hong[3,a], Hoang Nam Nhat[4], and Huynh Dang Chinh[1]

[1] School of Chemical Engineering, Hanoi University of Science and Technology, 1 Dai Co Viet, Hanoi, Vietnam
[2] Department of Material Engineering and Industrial Technology, University of Trento, v. Mesiano 77, 38050 Povo-Trento, Italy
[3] VNU University of Science, Hanoi, Vietnam
[4] Faculty of Technical Physics and Nanotechnology, VNU University of Engineering and Technology, Hanoi, Vietnam

Received: 3 January 2013 / Received in final form: 21 July 2013 / Accepted: 23 September 2013
Published online: 25 October 2013 –

Abstract. Mesoporous MgO has been synthesized in the presence of the neutral block co-polymer surfactant Pluronic F127. The characterization of synthesized material was carried out by mean of X-ray diffraction (XRD), scanning electron microscope (SEM) and Brunauer-Emmett-Teller technique (BET). The obtained MgO exhibited a value of the surface area of 157 m^2/g and showed a narrow pore size distribution centered at 4.3 nm. The phenomena and gas evolved during calcinations have been investigated by thermogravimeter-mass spectrometer (TG-MS). During the calcinations, the precursor $Mg(OH)_2$ was converted to MgO with a mass loss of 29% and with the formation of H_2O (>60% of the gas evolved). The desorption of CO_2 and a small amount of CO and/or N_2 which were adsorbed from air on the surface of $Mg(OH)_2$ were also observed. No organic compounds were found which indicated that F127 was completely removed by Soxhlet extraction.

1 Introduction

MgO was known as a promising basic catalyst and support additive for many catalytic reactions. As a typical electron donor material, MgO was frequently used as oxidation and dehydrogenation catalyst. The mixed catalysts of MgO such as V_2O_5/MgO for oxi-dehydrogenation of propane [1] and butane [2], Ni/MgO for CO_2 reforming of methane [3], CoMoS/MgO and NiMoS/MgO for the hydrodesulfurization of benzothiophene [4] have been studied. MgO can also be used as a chemical and destructive adsorbent for some toxic chemicals, such as chemisorptions of SO_2, destructive adsorption of organophosphonates [5–8] and chlorinated hydrocarbons [9]. The mesoporous MgO has been prepared various methods which include the sol-gel, hydrothermal, self-assembly, one-pot assembly of amphiphilic triblock copolymers and solvothermal methods [10–17]. However, the phenomena occurred during synthesis, especially during calcination stage, have not been fully explored in details. Therefore, this paper focuses on the phenomena occurred during the synthesis of MgO prepared in the presence of a neutral block copolymer surfactant Pluronic F127.

2 Experimental

In order to obtain 3 g MgO, 250 mL 0.5 M solution of $Mg(NO_3)_2$ (Merck, purity > 99.9%) was put into the reaction with 200 mL solution of NH_4OH (25–29%) (Sigma, purity > 99.5%) in the presence of 20 mL 5% solution of Pluronic F127 (Merck, purity > 99.9%) at room temperature in a sonic bath for 30 min. The precipitation of $Mg(OH)_2$ was washed and filtered in a centrifuge to remove NO_3^- ion. The remaining F127 was removed by a Soxhlet extraction using 500 mL ethanol in 6 h. Then obtained product was dried at 80 °C for 24 h. Finally, the dried $Mg(OH)_2$ was heated to 230 °C for 2 h, at calcined at 550 °C for the next 2 h to obtain mesoporous MgO (the heating rate was 0.5 °C/min). Thermogravimetric (TG) and differential thermal analyses (DTA) were performed on a LabSys Setaram thermobalance operating in the temperature range from 20 to 1000 °C, with a heating rate of 10 °C/min, under a 100 mL/min He flow. Typically, 20–40 mg of powdered samples was analyzed using a 100 μL alumina crucible and α-Al_2O_3 as reference. The gas species released from the solid sample during TG analysis were drawn into an alumina tube fixed inside the furnace of the thermobalance near the sample crucible and then connected to a capillary silica column heated at 300 °C. The gases were then directly sucked

* International Workshop on Advanced Materials and Nanotechnology 2012 (IWAMN 2012).

[a] e-mail: tthongkhcn@gmail.com

into the ionization chamber of the Carlo Erba Instrument QMD 1000 mass spectrometer. The specific surface area determination and pore size distribution were measured on an ASAP 2010 micromeritics apparatus. The N_2 adsorption was performed at −196 °C, evaluating the equilibrium points within a 0.05–0.33 p/p° range by the Brunauer-Emmett-Teller (BET) and Barret-Joyner-Halenda (BJH) equations. The XRD analyses were carried out at room temperature in the θ–2θ reflection mode using a D8 advance – Brucker diffractometer with Cu K_α radiation and a diffracted-beam graphite focusing monochromator. The intensity data were measured by a step scanning in the 2θ range from 10 to 70°, with 2θ step size of 0.05° and acquisition time of 2 s per point.

3 Results and discussion

3.1 MgO characterization

The crystalline phase of the mesoporous MgO can be clearly observed by XRD and SEM as given in Figure 1 (the SEM image of surface is given in the inset). It is worthwhile noting that three main MgO peaks appeared at 2θ = 36.9, 42.7 and 62.1° which correspond particularly to the reflection planes [1 1 1] [2 0 0] and [2 2 0]. The crystallite sizes along these directions, as calculated by the Sherrer's formula, were 11.7, 9.4 and 13.0 nm which averaged at 11.4 nm (Tab. 1). On the other hand, the SEM image (Fig. 1, inset) showed that MgO exhibits a form of rods with average polycrystallite grain diameter of 1 μm and length of 4 μm.

The nitrogen adsorption/desorption isotherm of the calcined MgO is shown in Figure 2. It is of a typical type IV (as defined by IUPAC) which shows a characteristic behaviour of a mesoporous material with hysteresis loop of type H3 [18].

The loop which does not exhibit any limiting adsorption at high p/p° was observed with aggregates of plate-like particles giving rise to the slit-shaped pores. The specific surface area was determined up to 157 m^2/g and pore volume of 0.70 cm^3/g. The pore size as calculated from the desorption branch by BJH method (shown in Fig. 2, inset) has narrow distribution over the range from 2.0 to 7.0 nm and is centered at 4.3 nm, indicating the fact that the corresponding mesoporous MgO has uniform pore size and meso-structure.

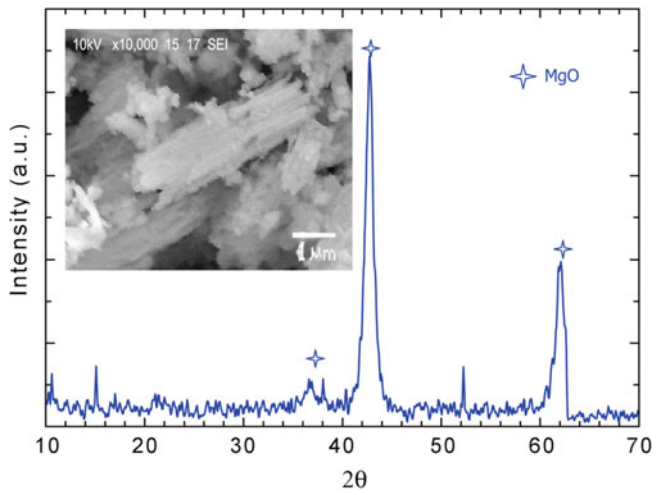

Fig. 1. The XRD patterns of the mesoporous MgO. The inset shows the surface image by SEM.

Table 1. The crystallite size (D) of mesoporous MgO as calculated by Sherrer's formula $D = 0.94\lambda/\beta\cos(\theta)$ (β is the full-width at half maximum, θ diffraction angle, λ wavelength).

2θ [°]	β [$\times 10^{-3}$ rad]	D [nm]/ref. plane
36.9	9.3	11.7/[1 1 1]
42.7	15.5	9.4/[2 0 0]
62.1	12.2	13.0/[2 2 0]

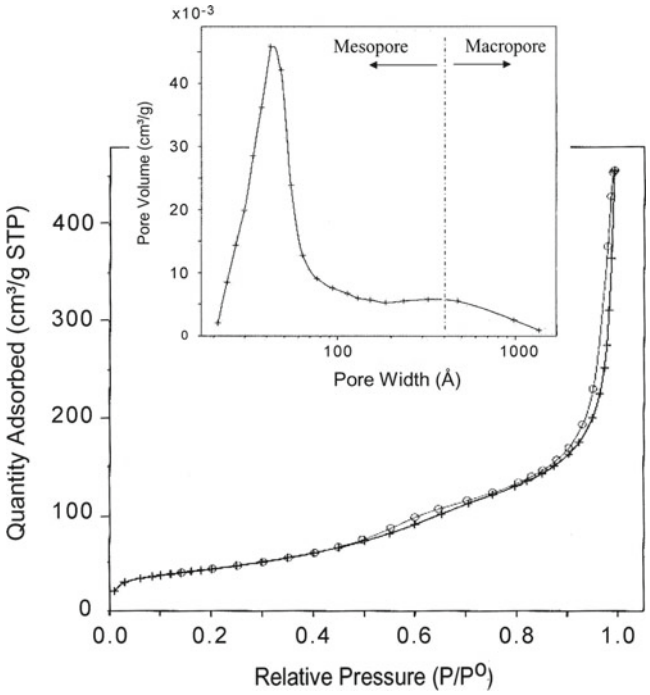

Fig. 2. N_2 adsorption and desorption isotherms of mesoporous MgO at 77 K. The inset shows the pore size distribution.

3.2 TG-MS analysis to understand the phenomena happens during calcinations

The TG-MS interface gives: (i) the graph of the total ion current (TIC), obtained from the contribution of all ions present in each recorded mass spectra, plotted vs. time, whose trend allows to detect any chemical species released from the sample; (ii) the plot of a selected mass to charge ratio m/z of ion current (IC), which could monitor the evolution of a single specific molecular species (during the whole pyrolysis), if this ion arises from the fragmentation pattern of that chemical species only; (iii) the integrations of the m/z ion currents vs. time, calculated by

the mass spectrometer software (in automatic or manual mode), yielding integrate values related to a quantitative information of those detected ion species [19].

As shown in Figure 3a, TG curve of dried $Mg(OH)_2$ presents one sharp mass loss up to 389 °C of a total loss of −26.75% intensity, followed by a 0.47% mass loss up to 480 °C and a 1.78% mass loss from 480 to 760 °C. The DTG curve shows one intense band at 389 °C and one sharp endothermic band also appeared in the DTA curve at 389 °C which corresponds to the decomposition of $Mg(OH)_2$ to MgO as follows:

$$Mg(OH)_2 \rightarrow MgO + H_2O \quad (1)$$

According to the stoichiometry of reaction, this reaction should lead to the mass loss of 31%. However it was only 26.75% in the TG result, so perhaps a part of dried $Mg(OH)_2$ was converted to MgO during the drying step. The evolved gas phase led to a TIC curve (Fig. 3b) which agrees with the trend seen in DTG: the sharp peak in the TIC curve at 39.04 min (around 389 °C) corresponds to the greatest mass loss during the pyrolysis. In TIC curve there are other two shoulders at 13.67 and 53.2 min. Mass spectra recorded in correspondence with the three TIC peaks at 13.67, 39.04 and 53.2 min are shown in Figure 4.

As observed, the mass spectrum at 39.04 min (∼389 °C) showed the main release of H_2O and CO_2 (with m/z of 18 and 44, respectively), whereas the spectra at 13.67 and 53.2 indicated the releases of H_2O, CO_2, CO and/or N_2 (with m/z of 28). While the water originated from the decomposition of $Mg(OH)_2$, the other gases such as CO_2, CO and/or N_2 were the adsorbed species from air on the surface of $Mg(OH)_2$. There was no trace of organic compounds observed and this indicated that the surfactant F127 was completely extracted by the Soxhlet extraction. So, during the dying and calcinations, the precursor $Mg(OH)_2$ was converted into MgO with the mass loss of approx. 29% and with the formation of H_2O

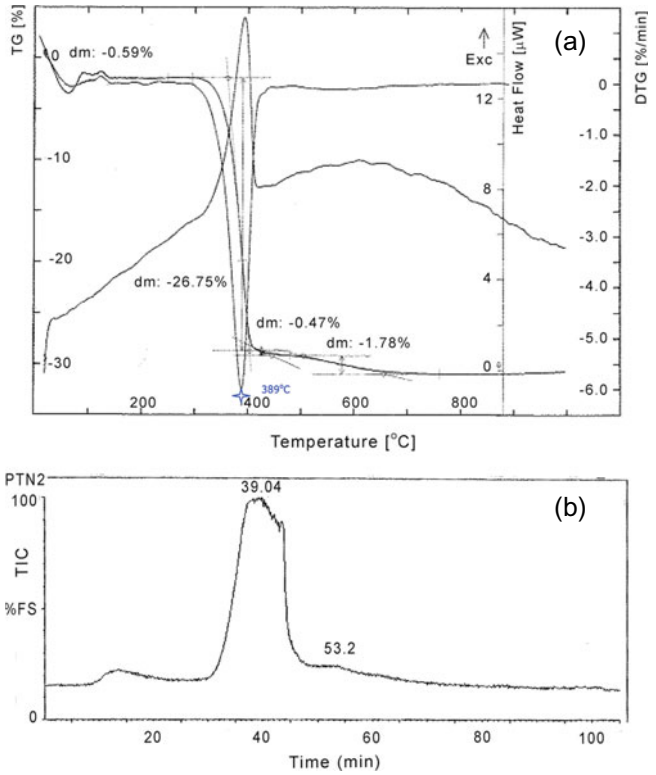

Fig. 3. (a) TG/DTG/DTA curves of $Mg(OH)_2$ (dried at 80 °C) and (b) total ion current (TIC) curve of evolved gases during the pyrolysis.

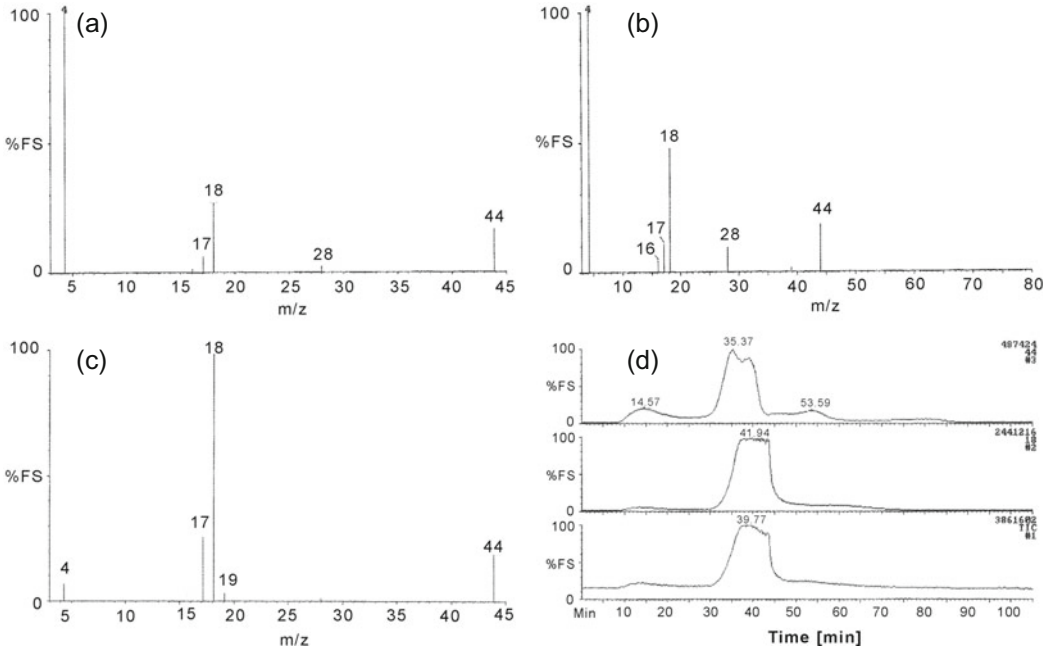

Fig. 4. Mass spectra recorded in the correspondence with three TIC peaks at (a) 39.04; (b) 13.67; (c) 53.2 min and (d) the formation of CO_2 and H_2O according to time on the stream.

(>60% of the gas evolved) and the desorption of CO_2 with a small amount of CO and N_2.

4 Conclusion

The processes of gas adsorption and desorption as well as the decomposition reactions evolved during thermal treatment of mesoporous MgO have been investigated by mean of TG-MS. The gas was composed mainly from CO_2 and H_2O (released as $Mg(OH)_2$ decomposed) and CO and/or N_2 which were adsorbed from air on surface of $Mg(OH)_2$. As demonstrated, the surfactant template F127 has been completely removed by Soxhlet extraction. The obtained mesoporous MgO nanocrystals possessed a large surface area of 157 m^2/g, with crystalline sizes ranging from 9 to 13 nm and a narrow pore size distribution around 4.3 nm.

This work was supported in part by University of Trento Italy – Vietnam mobility program. One of author (Hoang Nam Nhat) would like to thank the support from the National Foundation for Science and Technology Development of Vietnam (NAFOSTED), Project code #103.02.19.09 "Nanofluid and Application" (2009–2012).

References

1. C. Pak, A.T. Bell, T.D. Tilley, J. Catal. **206**, 49 (2002)
2. V.V. Chesnokov, A.F. Bedilo, D.S. Heroux, I.V. Mishakov, K.J. Klabunde, J. Catal. **218**, 438 (2003)
3. Y.-H. Wang, H.-M. Liu, B.-Q. Xu, J. Mol. Catal. A Chemistry **29**, 44 (2009)
4. T. Klicpera, M. Zdrazil, Appl. Catal. A **216**, 41 (2001)
5. K.J. Klabunde, J. Stark, O. Koper, C. Mohs, D.G. Park, S. Decker, Y. Jiang, I. Lagadic, D. Zhang, J. Phys. Chem. **100**, 12142 (1996)
6. J.V. Stark, D.G. Park, I. Lagadic, K.J. Klabunde, Chem. Mater. **8**, 1904 (1996)
7. E. Lucas, S. Decker, A. Khaleel, A. Seitz, S. Fultz, A. Ponce, W.F. Li, C. Carnes, K.J. Klabunde, Chem. Eur. J. **7**, 2505 (2001)
8. I. Muylaert, A. Verberckmoes, J. De Decker, P. Van Der Voort, Adv. Colloid Interface Sci. **175**, 39 (2012)
9. I.V. Mishakov, A.F. Bedilo, R.A.M. Volodin, V.I. Zaikovskii, J. Catal. **206**, 40 (2002)
10. D. Gulková, O. Šolcová, M. Zdražil, Micropor. Mesopor. Mater. **76**, 137 (2004)
11. A. Khaleel, P.N. Kapoor, K.J. Klabunde, Nanostruct. Mater. **11**, 459 (1999)
12. V.A. Hackley, P.K. Stoimenov, D.L. Ho, L.P. Sung, K.J. Klabunde, J. Appl. Cryst. **38**, 619 (2005)
13. M. Bhagiyalakshmi, J.Y. Lee, H.T. Jang, Int. J. Greenhouse Gas Control. **4**, 51 (2010)
14. Z. Ling, M. Zheng, Q. Du, Y. Wang, J. Song, W. Dai, L. Zhang, G. Ji, J. Cao, Sol. State Sci. **13**, 2073 (2011)
15. L. She, J. Li, Y. Wan, X. Yao, B. Tu, D. Zhao, J. Mater. Chem. **21**, 795 (2011)
16. S. Veldurthi, C.-H. Shin, O.-S. Joo, K.-D. Jung, Micropor. Mesopor. Mater. **152**, 31 (2012)
17. L. Ai, H. Yue, J. Jiang, Nanoscale **4**, 5401 (2012)
18. K.S.W. Sing, D.H. Everett, R.A.W. Haul, L. Moscou, R.A. Pierotti, J. Rouquerol, T. Siemieniewska, Pure Appl. Chem. **57**, 603 (1985)
19. R. Campostrini, M. Ischia, L. Palmisano, J. Therm. Anal. Calorim. **71**, 997 (2003)